IEEE TRANSACTIONS ON

INDUSTRY APPLICATIONS

A PUBLICATION OF THE IEEE INDUSTRY APPLICATIONS SOCIETY WWW.IEEE.ORG/IAS

SERVING OUR MEMBERS AND SUBSCRIBERS IN OUR FIFTY-FIRST YEAR OF PUBLICATION

NOVEMBER/DECEMBER 2015 VOLUME 51 NUMBER 6 ITIACR (ISSN 0093-9994)

PART II OF TWO PARTS

SPECIAL ISSUE ON GROUNDING SYSTEMS

(Contents Continued on Page 4877)

Digital Object Identifier 10.1109/TIA.2015.2499559

Analysis of High-Frequency Grounds: Comparison of Theory and Experiment

Robert G. Olsen, *Fellow, IEEE*, and Leonid Grcev, *Fellow, IEEE*

***Abstract*—To date, there has not been a completely satisfactory comparison between theory and experiment for a ground system that is excited by a current with a submicrosecond rise time. This requires careful definitions of both the measured and calculated voltages because the electric field is no longer conservative and voltages become path dependent. An experiment performed by EdF in the late 1970s has been carefully analyzed and compared with a simulation using full-wave theory. The comparison is excellent, and this example can now be used as a "gold standard" to which approximate grounding theories can be compared.**

***Index Terms*—Electrical safety, grounding, power system simulation, substation protection, transmission lines.**

I. Introduction and Background

TRANSMISSION line towers are "grounded" to provide a low-impedance path for abnormal currents that may appear on transmission lines due to either lightning or faults. It is important to realize that, during these events, the "earth" is not at constant potential. In fact, there can be lethal potential differences between different parts of the earth that pose serious safety concerns for individuals who are in the vicinity of these "grounds." In addition, sensitive equipment can be exposed to transient voltages high enough to cause damage.

Grounding systems are often analyzed using quasi-dc methods. However, it is not always clear whether this type of analysis can be correctly applied to ground systems for which the dimensions of the ground are not small compared with the highest wavelength (in the earth) of the current injected into the ground system. The purpose of this paper is to explore the case for which the ground system cannot be analyzed using quasi-static theory and to illustrate the effectiveness of appropriate high-frequency analysis by comparison of both high-frequency and quasi-dc analysis to a carefully conducted and interpreted experiment.

Classical analysis of grounding systems basically has two goals: first, to represent the grounding system by an equivalent circuit, which can be introduced in overall circuit analysis of the system during abnormal conditions, and, second, to determine voltages in the vicinity of the ground, which have to be reduced within safe limits. At dc and low frequencies (which includes normal 50-/60-Hz regime and, often, system faults), the equivalent circuit is simple, and voltages are unique and equal to potential differences. Behavior of grounding systems in such low a frequency regime is well understood and is regulated in standards, for example, [1]. However, dynamic behavior in case of intensive and fast-varying currents, such as in case of lightning strokes, might be quite different. Fast-varying currents contain high frequencies for which grounding systems often cannot be represented only by resistors, and currents with high intensity often give rise to nonlinear ionization of the earth.

Pioneering but comprehensive work on this subject was conducted in the first half of the 20th century [2]–[4]. Classical modeling approaches are based on circuit or transmission line theory, where grounding electrodes are represented by equivalent lumped or distributed resistances, inductances, and capacitances, as derived from quasi-dc analyses. They were first applied to single straight grounding electrodes, for example, in [5]–[7]. Recently, using computers, circuit models have been extended to model complex grounding systems [8]–[11]. However, the validity of these models is limited to a certain upper frequency, due to underlying quasi-dc approximations.

Full-wave modeling methods without frequency limitations have been also introduced, based on the solution of the integral form of Maxwell equations [12]–[15]. Such electromagnetic models are based on an exact mathematical formulation that is numerically solved using the method of moments originally developed for antenna theory [16].

Classical experimental work was mostly focused on the effects of ionization in the earth due to direct lightning strokes [17]–[20]. There is a lack of carefully documented experimental work in the available literature, of which noteworthy recent exceptions are [21]–[24]. Most experimental work has been done for current pulses with front times larger than 1 μs that are typical for first lightning strokes, only a very small number for submicrosecond pulses that are typical for subsequent strokes.

The most important part of the modeling is the validation of the models in comparison with experimental results. However, there has been no complete comparison between theory and experiment for submicrosecond pulses. One of the reasons for the lack of comparison is that high-frequency voltages are difficult to define uniquely. Here, a careful definition of "voltage" is given and applied both to the theory and to the system used to measure voltage during the experiment. When consistent definitions are used, the result is a successful comparison.

Manuscript received December 13, 2014; revised February 2, 2015; accepted February 4, 2015. Date of publication March 6, 2015; date of current version November 18, 2015. Paper 2014-PSEC-0903.R1, approved for publication in the IEEE TRANSACTIONS ON INDUSTRY APPLICATIONS by the Power Systems Engineering Committee of the IEEE Industry Applications Society.

R. G. Olsen is with the School of Electrical Engineering and Computer Science, Washington State University, Pullman, WA 99164 USA (e-mail: bgolsen@wsu.edu).

L. Grcev is with the Faculty of Electrical Engineering and Information Technologies, Ss. Cyril and Methodius University, Skopje 1000, Macedonia, and also with the Macedonian Academy of Sciences and Arts, Skopje 1000, Macedonia (e-mail: Leonid.Grcev@ieee.org).

Color versions of one or more of the figures in this paper are available online at http://ieeexplore.ieee.org.

Digital Object Identifier 10.1109/TIA.2015.2409271

It will be assumed here that the earth is a linear, homogeneous, and isotropic medium. However, it has been known for many years that, if the electric field (and hence current density since $\overline{J} = \sigma \overline{E}$) in the earth is large enough, the soil becomes ionized, and the earth effectively becomes a nonlinear medium [25]. Furthermore, the effective resistivity in the ionized region is decreased, hence decreasing the grounding resistance of the earth [18]. Experiments by different researchers suggested that threshold for soil ionization can be in the range from less than 1 to more than 10 kV/cm [26], [27]. Analyzing a large number of experimental data, Mousa suggested 3 kV/cm as a suitable value for the threshold for soil ionization to be used in theoretical evaluations [28]. Recent work in developing nonlinear models in this area has been reported by Cooray [29]. The interested reader may refer to [30] for a discussion on how this influences the ground system and how the theory reported here can be extended to account for this phenomenon.

It is important to note that the ionization of the soil, which is typical for high current intensities, may improve the impulse grounding performance, and neglect of this phenomenon leads to conservative results. On the other hand, during fast rise time currents, inductive effects may lead to deterioration of the grounding performance, with possible large transient voltages, which should not be neglected. These effects are the focus of this paper. As noted earlier, the essential contribution of this paper is the careful analysis of an experiment using a simple grounding system driven by an impulse current with a submicrosecond rise time.

II. Overview of the EdF Experiment

Over a 15-month period from late 1976 to early 1978, a number grounding system experiments for short rise time input current pulses were conducted by EdF in Les Renardieres, France [31]–[33]. The specific case of interest here (see [32, Fig. 3–16b]) is the case for a 15-m-long horizontal copper wire ground electrode that has a 6-mm radius and is buried 0.6 m eep in earth with resistivity ρ_e and relative permittivity ε_r in the range of 70 $\Omega \cdot$ m and 15, respectively. A schematic of the electrode and the equipment used to perform the experiment is shown in Fig. 1.

The endpoint of the wire was driven by a 20-kV surge generator that injected a current pulse with a maximum amplitude of 33 A and a zero-to-peak rise time of approximately 0.8 μs through a 500-Ω matching resistor into the wire. The "voltage to ground" was measured across a 1-Ω load resistor (Z_L) at the termination of a 15-m-long resistive divider, 1.2 m above the ground. The input of the divider was connected to the driving point of the ground system (G) by a 2-m-long horizontal connection wire. Its length was oriented perpendicular to the buried ground wire, as illustrated in Fig. 1(b) [34] and hence was not subject to magnetic induction from current in the buried ground wire. Details of the surge generator design are shown in Fig. 1(c) [35]. For the pulse used in this study, $v_g(t)$ was a step pulse with a rise time of 1 ns and was connected to the pulse-forming circuit by a coaxial cable with a characteristic impedance Z_0 of 12.5 Ω. The values of the pulse-forming resistor R_g and capacitor C_g were 350 Ω and 250 pF, respectively;

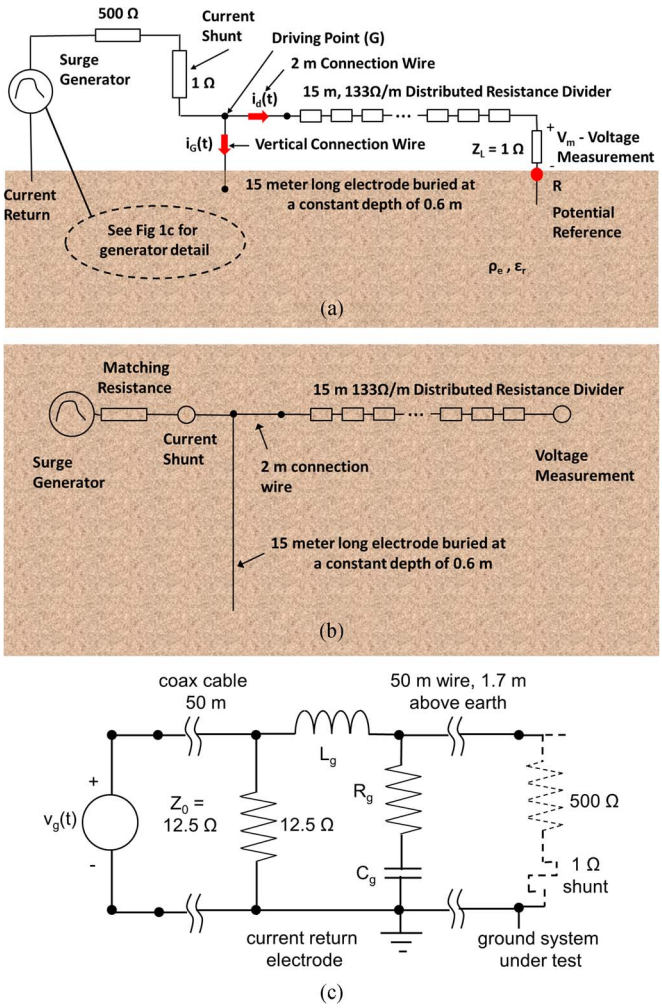

Fig. 1. Electrode under test and the experimental setup. (a) Side view. (b) Top view. (c) Detail of the surge generator circuit (circuit values in text).

whereas L_g consisted of 60 turns of wire with a 5-mm^2 cross-sectional area wound on a 100-mm-diameter insulating tube [35]. Different pulse types can be constructed using different values of R_g, C_g, and L_g. This pulse generator was used to drive the ground system through a 50-m-long wire, 1.7 m above the earth. Several orientations of the current-carrying wire were tried, and the best results were obtained with a wire in line with the resistive divider and therefore perpendicular to the buried ground wire [35].

The current at the input to the ground system (measured using a 1-Ω current shunt) and the current at the input to the resistive divider system are $i_G(t)$ and $i_d(t)$, respectively, as shown in Fig. 1(a). The point to which voltages will be referenced is labeled as "R."

The results of the current and voltage measurements are shown in Fig. 2(a) and (b), respectively. In addition, a simulation of the voltage using quasi-dc grounding theory is shown in Fig. 2(b). Clearly, this quasi-dc theory is not adequate to calculate the "short-time" voltage response of this ground system for injected currents with submicrosecond rise times. The reason for this failure is the focus of this paper. More specifically, the purpose of the paper is as follows: to identify a "dynamic" theory that can be used to effectively simulate

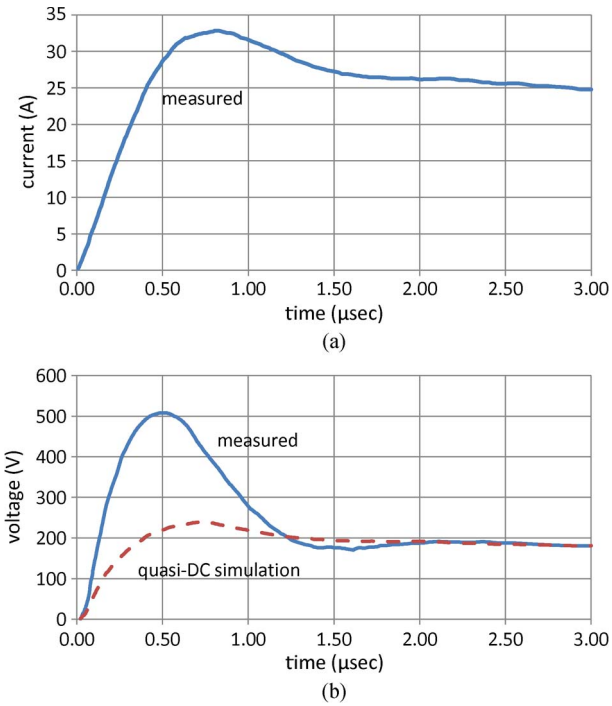

Fig. 2. Measured current $i_G(t)$ and voltage $v_{\rm GR}(t)$ for the EdF experiment along with simulated quasi-dc voltage calculation. (a) Current. (b) Voltage. Details about how the measurement was made will be discussed shortly.

this ground system and to carefully study the question of how properly conducted and interpreted simulations of voltage can be compared with the results of properly conducted and interpreted "short rise time" ground response experiments for the entire duration of the current pulse. This work will be described in the subsequent sections.

A. Initial Comments on the Measured Voltage and Current

It is first noted that the main difference between the measured voltage and the quasi-dc simulation is the voltage peak that occurs within the first microsecond of the response. This peak has shorter zero-to-peak rise time than that of the current (i.e., approximately 0.5 μs versus approximately 0.8 μs). Furthermore, as will be discussed shortly, the response of the ground system is consistent with modeling the ground system as a simple inductor for early times. Using the measured data in Fig. 2 for the 90%–10% of full voltage across the inductor, the inductance is

$$L = \frac{v - iR_{\rm dc}}{di/dt} = \frac{240\ \text{V}}{60\ \text{A}/\mu\text{s}} \cong 4.0\ \mu\text{H}. \tag{1}$$

At later times, the measured data and the quasi-dc simulation are in agreement as shown.

III. Self-Consistent Recovery of the Earth Resistivity

It is clear from Fig. 2 that traditional quasi-dc methods are not appropriate for short time analysis of ground systems with submicrosecond rise times. As pointed out earlier, however, the current and voltage stabilize for longer times and approach the dc solution for which the input impedance is purely resistive. These "asymptotic" values can be used in conjunction with quasi-dc theory to determine the earth's resistivity.

Consider the horizontal ground system shown in Fig. 1 that was used in the EdF experiment. The buried conductor is connected to the earth's surface at one end by a vertical length of conductor of the same radius, which has a current $i_G(t)$ injected into it at the earth's surface. The "late-time" voltage can be found using any one of many different quasi-dc grounding programs [36]–[38]. These programs calculate the grounding resistance R_g, which is equal to the voltage divided by the input current. Programs to be described later that account for the dynamics are required for determining inductance values. To be consistent with the experiment, the calculated quasi-dc voltage is defined as the difference in potential between driving point (G) of the ground system and a reference point R in Fig. 1 that is 17 m from G in a direction perpendicular to the horizontal ground wire. Note that, here, the reference is not "remote earth" as often used because the intent is to compare the simulation with the experiment, which uses the potential reference point R shown in Fig. 1. Given the geometry of the experiment, $R_{\rm GR}$ (the late-time ground "resistance") represents the late-time voltage between the driving point (G) electrode and the reference point (R) divided by the late-time input current $i_G(t)$.

The late-time data shown in Fig. 2 can now be used to determine the appropriate earth resistivity because they can be determined using knowledge of ground system geometry and resistivity of the earth alone. From Fig. 2, $R_{\rm GR} = 180.9\ \text{V}/24.8\ \text{A} = 7.3\ \Omega$. Using a quasi-dc ground system analysis program, $R_{\rm GR}$ was calculated a number of times with different values of earth resistivity until the value obtained was $R_{\rm GR} = 7.3\ \Omega$. The result of this calculation was an earth resistivity $\rho_e = 79\,\Omega \cdot \text{m}$, which was used in all subsequent analysis.

By deriving the value of earth resistivity from the same experiment to be analyzed dynamically, a "self-consistent" earth resistivity was obtained. This removed the need to use an independent experiment that might have been conducted at a different time under different weather conditions and produced a different value of resistivity.

The value of the relative dielectric constant of the earth was selected (somewhat arbitrarily) to be 15. However, sensitivity studies have shown that, for the low-resistivity soils relevant to the EdF experiments, the specific value has relatively little impact on the result.

Using $R_{\rm GR} = 7.3$, an application of quasi-dc theory to this experiment results in a voltage equal to

$$v_{\rm GR}(t) = R_{\rm GR} i_g(t) = 7.3 i_g(t) \tag{2}$$

and is plotted in Fig. 2(b).

IV. Introduction to the Need for High-Frequency Analysis

Because the match between the measured data and the quasi-dc simulation is not good for early times, it is to be expected that a high-frequency (or dynamic) model is needed. Such models

Fig. 3. Equivalent circuit for the simple ground system model that accounts for inductive effects and is useful for predicting some aspects of early-time transient voltages across grounding systems.

have been available for some time [2], [4]. One simple circuit model that has been able to provide better results for higher frequencies than a simple grounding resistance R_g is shown in Fig. 3. It includes an inductance L_g in series with R_g.

The effect of the inductance can be illustrated by injecting a current pulse of the form

$$i_G(t) = I_{\max}\left(1 - e^{-bt^2}\right) \tag{3}$$

into the equivalent circuit for simple ground system model, where "b" is a parameter that determines the rise time of the pulse.

For this current, the voltage across the circuit (i.e., to "ground") is

$$v_{\rm GR}(t) = I_{\max}\left\{(2btL_g - R_g)e^{-bt^2} + R_g\right\}. \tag{4}$$

Note that, if $\mathrm{b} \to 0$ (i.e., a very slow rise time)

$$v_{\rm GR}(t) = R_g I_{\max}\left(1 - e^{-bt^2}\right) \tag{5}$$

which is the quasi-dc solution as expected. Now, if

$$\sqrt{b}L_g > R_g/\sqrt{2} \tag{6}$$

there is an early-time peak in the voltage, which can be shown to have a maximum value at $t_{\max} = \sqrt{1/2b}$ of

$$v_{\max}\left(t = \sqrt{1/2b}\right) = I_m\left\{\left(\sqrt{2b}L_g - R_g\right)e^{-1} + R_g\right\}. \tag{7}$$

Clearly, the rise time required to result in such a peak is smaller in ground systems with larger ground resistances. This can happen either because the earth has a higher resistivity or because the ground system is not extensive and hence has a relatively large value of R_g. It is interesting to note that, as R_g is made smaller by improving the ground system, the final voltage may be made smaller, but the initial voltage may increase due to this inductive effect. This is an example of a "tradeoff" between late- and early-time performance when "better" (i.e., low-resistance) grounds are designed. On the other hand, if

$$\sqrt{b}L_g < R_g/\sqrt{2} \tag{8}$$

there is no maximum, and the effect of the inductance is significantly less. In fact, as $\mathrm{b} \to 0$, the solution reduces to the quasi-dc solution as illustrated in (5). Hence, for pulses with longer rise times, the effect of inductance can often be ignored, and the ground can be represented simply by the grounding resistance.

Examples of a current pulse with a submicrosecond rise time and the resulting transient voltage across the ground system are shown in Fig. 4. To be as consistent with the EdF experiment

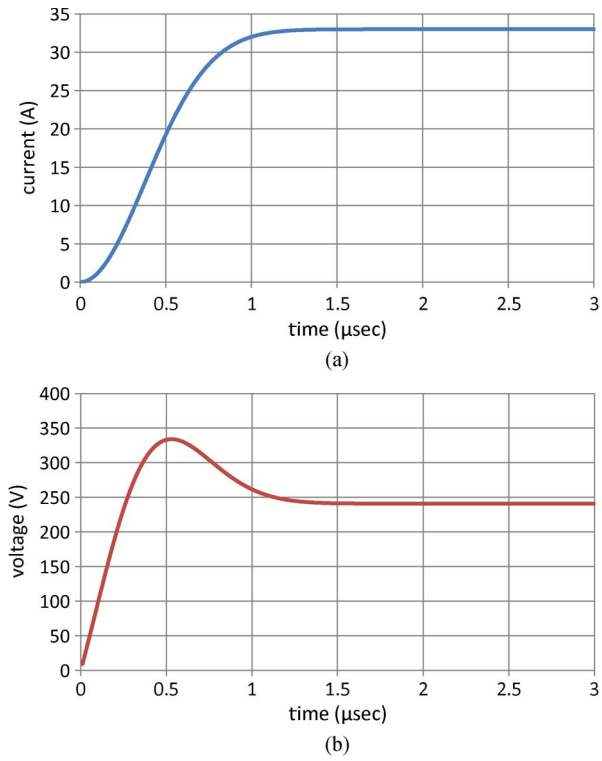

Fig. 4. Current injected into and voltage across a grounding system modeled as an inductance in series with a grounding resistance. Here, $I_m = 33$ A, $b = 3.5 \times 10^{12}$, $R_g = 7.3\ \Omega$, and $L = 6.4\ \mu$H. (a) Current. (b) Voltage.

as possible, the parameters $I_m = 33$ A, $\mathrm{b} = 3.5 \times 10^{12}$, $R_g = 7.3\ \Omega$, and $\mathrm{L} = 4.0\mu\mathrm{H}$[1] have been used.

Clearly, Fig. 4 is not an adequate simulation of the experimental results shown in Fig. 2. Nevertheless, the results shown in Fig. 4 illustrate the initial peak in the early-time voltage and the asymptotic values of the late-time current and voltage. The most serious barrier to using this simple approach is that there is no generally accepted method for a priori calculating the inductance of buried wires. Hence, the simulations used here implement the full-wave theory to be discussed further later in this paper. It is clear that the inductance can cause a significant voltage overshoot for submicrosecond pulses injected into grounding systems with typical inductance and resistance values. While these voltage pulses are relatively short, they may still be of concern for human safety and may pose a threat to equipment with earth connections.

This initial overshoot behavior is evident in the experimental results presented earlier. Hence, the addition of inductance to the model appears to be the most important improvement that can be made. The full-wave model used here to simulate the experimental results certainly includes the inductive effects described here, but since it is an exact theory, it also includes capacitive and propagation effects as well.

[1]The value of L used here is from the experimental result shown in (1). It has been used because there does not appear to be a well-accepted method for accurately calculating the external inductance of a buried wire carrying a nonuniform current for high-frequency ground models [39], [40]. Issues range from the nonuniqueness of partial inductance calculations to the nonfiniteness of magnetic energy associated with currents that do not form closed loops.

V. On the Definition of Voltage

A. Introduction

The specific issue to be considered here is the difficulty in defining voltage at higher frequencies when the distance over which a voltage is defined is not a very small fraction of a wavelength and hence the electric field cannot be considered conservative. Hence, any potential defined here must be path dependent, and the path must be defined. Here, a careful examination is made of both the definition used to calculate the ground system voltage and the method by which this voltage was measured in the experiment. The purpose of this examination is to be certain that these are carefully and equivalently defined. Without this equivalence, it is not possible to compare experiment and theory.

B. Voltage to Remote Earth

It is common to characterize a ground system by its driving point impedance.[2] This impedance is defined as the voltage between (some) two terminals divided by the current between the same two terminals. It generally is not difficult to define the terminal into which the system current flows and which forms one of the terminals between which the voltage is defined. It is also not difficult to define the voltage "if" the two terminals between which the voltage is defined are very close to each other compared with a wavelength. However, it is difficult to define the voltage in the way that it has traditionally been defined for grounding electrodes at dc (i.e., with respect to remote earth, which is an infinite distance away) because, at higher frequencies, these two terminals are not close compared with a wavelength. Furthermore, the second terminal for the voltage measurement may not be the one that collects all of the current that flows into the grounding system.

Here, the issue is resolved by defining the first terminal as the driving point of the ground system, the current as that which flows into this terminal, and the voltage at this terminal with respect to a known reference point (R) at a finite distance from the ground system driving point rather than with respect to remote earth. As long as the reference point is the same for both experiment and theory, there should be no difficulty with this assumption.

C. Use of Contour-Dependent Voltages

A second (and related) issue with the definition of voltage is that voltage is path dependent for a general time-varying electric field. Consider the situation illustrated in Fig. 5, where the input terminal of the ground system is labeled G, and the voltage reference point is labeled R. Here, an attempt is made to define the voltage at high frequency between the corner of a buried mesh electrode and reference point R along one of two paths: Path GR_1 or Path GR_2. According to Faraday's law, the difference in the voltages between the mesh corner and the "reference" terminal along Path GR_1 and Path GR_2 is equal to the time rate of change of magnetic flux through the surface S bounded by the closed path C that consists of Path GR_1, followed by Path GR_2, but traversed in the opposite direction. More specifically,

$$\oint_C \overline{E} \bullet d\bar{l} = \int_{GR_1} \overline{E} \bullet d\bar{l} - \int_{GR_2} \overline{E} \bullet d\bar{l} = -j\omega \int_S \overline{B} \bullet d\bar{S}. \quad (9)$$

If the magnetic induction term on the right side is small compared with the calculated voltage along either path, then it is reasonable to define a voltage. Grcev and Arnautovski-Toseva, however, showed one example for which there is a significant difference in the voltage calculated along two paths for a grounding electrode that is excited by the subsequent stroke of a lightning impulse. Hence, the definition of potential must include the path, and care must be taken when defining the path used for the potential [42].

This idea can be applied to the measurement system for the EdF experiment, as shown in Fig. 6. Here, a closed contour containing points G and P is shown as the dashed red rectangle. Note that the rectangle could be any rectangle that fits inside the boundaries of the ground feed, the earth, and the measurement system. One specific case of interest, for example, is the rectangle such that P = R, the reference point used to analyze this ground system's voltage.

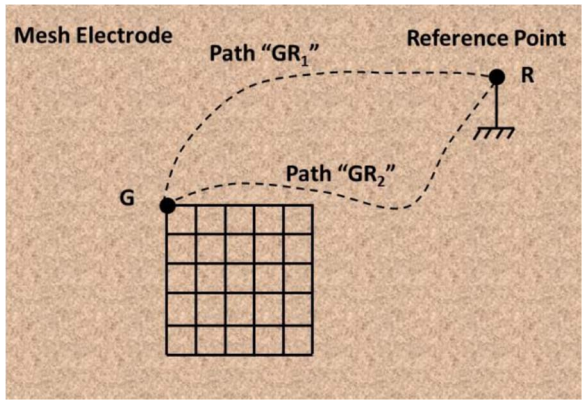

Fig. 5. Mesh electrode is shown with two paths to a point far enough from the electrode that is the "reference point."

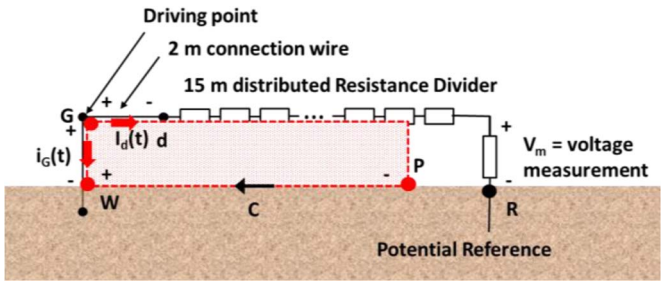

Fig. 6. Contour in the plane of the resistive divider for which magnetic induction from the horizontal ground wire is zero.

[2]It is noted that the term "impedance" is used quite loosely in many (if not all) high-frequency grounding theories for just the reason discussed earlier; the voltage is not uniquely defined at higher frequencies. In fact, quantities termed impedance (i.e., transient impedance, impulse impedance, and harmonic impedance) should not be considered as well-defined impedances since corresponding voltages in their definitions are not voltages between the current source terminals, but only potentials at the grounding electrode feed point [41].

The magnetic fields generated by currents in the buried horizontal ground wire are parallel to the surface S of the rectangle shown in Fig. 6. Hence, there is no magnetic induction through S from these buried currents. However, there is magnetic induction from currents in the vertical wire that connects the driving point and the earth and the horizontal connection wire.[3] These will be accounted for as lumped self-inductances, as shown in

$$-\oint_C \overline{E} \bullet \bar{d}\,\bar{l} = 0 = -\int_P^W \overline{E} \bullet \bar{d}\,\bar{l} + j\omega L_{\rm vw}\hat{I}_g \; - j\omega L_{\rm hw}\hat{I}_d + \int_P^d \bar{E} \bullet \bar{d}\,\bar{l} \qquad (10)$$

where the subscripts vw and hw refer to the vertical and horizontal wires, respectively.

It is further recognized that any electric field can be written in terms of vector magnetic and scalar electric potentials, i.e.,

$$\hat{\overline{E}}(\omega) = -\nabla\hat{\phi}(\omega) - j\omega\hat{\overline{A}}(\omega) \qquad (11)$$

where $\hat{\overline{A}}$ is the vector magnetic potential, and $\hat{\phi}$ is the corresponding electric scalar potential.

Given this,

$$\int_P^W \nabla\hat{\phi}(\omega) \bullet \bar{d}\bar{l} = \hat{\phi}_{WP}(\omega) = -\int_P^W \overline{E}(\omega) \bullet \bar{d}\,\bar{l} - \int_P^W \bar{A}(\omega) \bullet \bar{d}\,\bar{l} = -\int_P^W \overline{E}(\omega) \bullet \bar{d}\,\bar{l} \qquad (12)$$

with the reference direction shown in Fig. 6. Note that $\hat{\overline{A}}(\omega) \cdot \bar{d}\bar{l} \cong 0$ on the contour along the earth's surface that connects G and P since the current in the ground system is perpendicular to it and the magnetic flux due to the currents in the vertical wire and the measurement lead are accounted for by their self-inductances. This self-inductance of the measurement wire can, in turn, be neglected, as shown in the next section. The potential $\hat{\phi}_{WP}(\omega)$ is uniquely defined for the contour along the earth's surface in Fig. 6. Furthermore, this is the "potential" that reduces to the normal electrostatic potential as the frequency goes to zero or for which there is no (or very little) time variation of the fields.

The simulated voltage calculated is

$$\hat{V}_{\rm GR}(\omega) \; = j\omega L_{\rm vw}\hat{I}_g(\omega) + \hat{\phi}_{WR}(\omega) \qquad (13)$$

where the point R has now been used as the reference. $\hat{\phi}_{WR}(\omega)$ is calculated by the simulation program as the negative integral of the electric field along the path from R to W. In the next section, the measured voltage will be defined. Care must be exercised to be certain that the definitions of "measured" and "simulated" voltages are consistent.

[3]The magnetic induction due to the horizontal resistive divider can be ignored because (as shown later) the resistance of this portion of the measurements system dominates its self-inductance.

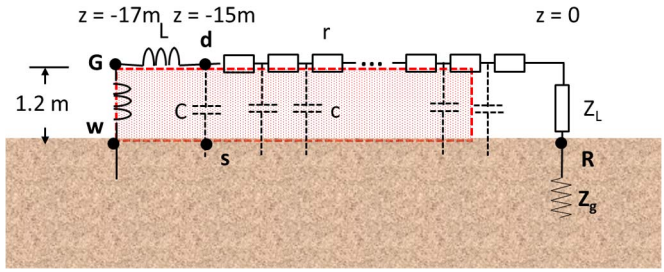

Fig. 7. Measurement system showing distributed parameters.

VI. Interpretation of the EDF Experiment

According to Grcev and Fieux *et al.*, the measured voltage in the EdF experiment was obtained in the following way. The "transient voltage to *remote ground*[4] has been measured by means of a 15 m long[5] ohmic divider with measuring bandwidth of 3 MHz. The high voltage arm was composed of a series of ceramic resistances connected to very short connectors. By employing this measuring arrangement, a constant transfer function in the measuring bandwidth could be realized." [34], [43].

The goal of this measurement is to find the voltage at G with respect to the potential reference R so that the measured voltage is consistent with (13). However, as is apparent from the measurement defined in Fig. 1, the voltage that has actually been measured is not $\hat{V}_{\rm GR}(\omega)$ but the voltage $\hat{V}_m(\omega)$ across a 1-Ω resistor at the end of the distributed resistive divider. The relationship between $\hat{V}_m(\omega)$ and $\hat{V}_{\rm GR}(\omega)$ must be carefully defined.

A. Defining the Measured Voltage

Before analyzing the voltages, a circuit model for the measurement system (a distributed resistive divider) will be examined more carefully. Consider the measurement system shown in Fig. 7. At higher frequencies, the inductances of straight wires and capacitance to ground of the horizontal wires must be considered and are shown. The horizontal connection wire between G and d can be represented as a series inductance of 2 μH/m $\times$ 2 m $=$ 4 μH and a shunt capacitance of 10 pF/m $\times$ 2 m $=$ 20 pF [34]. The vertical connection wire between G and w can be represented as an inductance of 1.2 μH [44]. The inductance between the circuit injection and the voltage measuring arms of the measurement system can be computed to be in the range of about 0.16 μH and therefore can be neglected in the computation of the voltage.

The distributed resistance divider can be modeled as a lossy transmission line characterized by a series impedance per unit length that consists of a resistance and an inductive reactance per unit length, i.e.,

$$z = r + j\omega l \cong r \qquad (14)$$

[4]The voltage was measured with respect to the reference point "R," not "remote earth.

[5]Grcev in [43] stated a length of 60 m here, but in the original reference, 15 m was used.

TABLE I
DISTANCE TO EFFECTIVE GROUND REFERENCE POINT FOR FREQUENCY COMPONENTS OF $\hat{\phi}_{\rm GR}(\omega)$

Frequency	Distance from entry point to $0.95\hat{\phi}_{WR}(\omega)$
100 Hz	22.6 meters
100 kHz	5.9 meters
1 MHz	2.6 meters
3 MHz	1.5 meters
5 MHz	1.1 meters

and the parallel admittance per unit length of the distributed resistance divider is capacitive and equal to

$$y = +j\omega c \tag{15}$$

where $c = 10$ pF/m.

The approximation in (14) is valid because the value of r used in the experiment was 133 Ω/m, and since the value of l used in the experiment was 2 μH/m, the value of $j\omega l$ at 3 MHz (largest frequency of interest) is only approximately 38 Ω/m. Hence, the term $j\omega l$ can be neglected.

It will be convenient to analyze the measurement problem first in the frequency domain and then to transform back to the time domain for the following reason. As aforementioned, the potential difference $\hat{\phi}_{WR}(\omega)$ is defined here with respect to the reference point R in Fig. 7. However, as will be illustrated shortly, at high frequencies, the integral used to calculate $\hat{\phi}_{WR}(\omega)$ converges well before the point R is reached, and it is possible to identify a point on the ground closer to W as the "effective" reference point (for that frequency) without affecting the value of the potential. This can be illustrated by examining the convergence of calculations of $\hat{\phi}_{WR}(\omega)$ at different frequencies. More specifically, the distances (for a number of frequencies) from the point W at which the integral for $\hat{\phi}_{WR}$ has "converged" (i.e., 95% of the final value) have been calculated and are summarized in Table I.

At 100 Hz, the calculation of $\hat{\phi}_{WR}(\omega)$ requires the full range from W to R. However, at higher frequencies, the integral converges well before the point R. Hence, at 100 kHz, for example, the region from 5.9 m to R contributes little to $\hat{\phi}_{WR}(\omega)$, and it can be argued that an equivalent reference point for $\hat{\phi}_{WR}(\omega)$ is 5.9 m from W.

Furthermore, at 1 MHz, it can be argued that the reference point is 2.6 m from W and that the integration path beyond that contributes little. At higher frequencies, convergence occurs even closer to W. As will be illustrated shortly, there is utility to recognizing that, at high frequencies, essentially all of the contributions to the integral $\hat{\phi}_{WR}(\omega)$ come from close to the point at which the ground system enters the earth (i.e., W) so that

$$\hat{\phi}_{WR}(\omega) \cong \hat{\phi}_{Ws}(\omega) \quad \text{(at high frequencies)} \tag{16}$$

where $\hat{V}_{ds}(\omega)$ is the input voltage to the distributed resistive divider between terminals d and s, and $\hat{V}_{Ws}(\omega)$ is the input voltage to this divider between terminals W and s when augmented by the equivalent circuit for the connection wire. What happens at lower frequencies will be discussed shortly.

Including the inductive and capacitive effects of the horizontal connection wire, the transfer function $H(\omega)$ between the measured voltage V_m at the output of the measurement system and the input voltage to the measurement system V_{Gs} can be written as

$$\frac{\hat{V}_m(\omega)}{\hat{V}_{Gs}(\omega)} = H(\omega) = |H(\omega)|\, e^{j\theta(\omega)} = \frac{(1+\Gamma)\, Z_0}{den} \tag{17}$$

where

$$\begin{aligned} den = {} & \left(j\omega L_h + Z_0(1-\omega^2 L_h C_h)\right) e^{j\gamma\ell} \\ & - \Gamma \left(j\omega L_h - Z_0(1-\omega^2 L_h C_h)\right) e^{-j\gamma\ell} \end{aligned}$$

$$\Gamma = \frac{Z_L - Z_0}{Z_L + Z_0}, \tag{18}$$

$$j\gamma = \sqrt{zy} \cong \sqrt{jr\omega c} = e^{j\pi/4}\sqrt{\omega r c} \tag{19}$$

$$Z_0 = \sqrt{\frac{z}{y}} \cong \sqrt{\frac{r}{j\omega c}} = e^{-j\pi/4}\sqrt{\frac{r}{\omega c}}. \tag{20}$$

Z_L is the load impedance that includes the 1-Ω shunt resistor and the "grounding impedance Z_g"; whereas L_h and C_h are the inductance and the capacitance, respectively, of the horizontal connection wire.[6] "s" is the point on the earth directly below the input to the resistive divider, as shown in Fig. 7.

Now, for all frequencies of interest here (i.e., conservatively for frequencies less than approximately 3 MHz), the terms containing L_h and C_h can be ignored. Hence

$$H(\omega) \cong \frac{(1+\Gamma)}{e^{j\gamma\ell} + \Gamma e^{-j\gamma\ell}}. \tag{21}$$

This expression is simplified if (18) is used in (21) to obtain

$$H(\omega) \cong \frac{Z_L}{jZ_0 \sin(\gamma\ell) + Z_L \cos(\gamma\ell)} \cong \frac{Z_L}{jZ_0 \sin(\gamma\ell)} \tag{22}$$

since, for the parameters used in this problem, $Z_L \ll |Z_0 \sin(\gamma\ell)|$.

If further, $\sin(\gamma\ell)$ is expanded in a two-term Taylor series, i.e.,

$$\begin{aligned} H(\omega) &\cong \frac{Z_L}{jZ_0\gamma\ell\left(1 - \frac{(\gamma\ell)^2}{6}\right)} \\ &= \frac{Z_L}{r\ell\left(1 + j\omega\left(\frac{rc\ell^2}{6}\right)\right)} \left(\omega r c \ell^2\right)/6 < 1. \end{aligned} \tag{23}$$

The parameters used here are [34] as follows: $\ell = 15$ m; $r = 2000/15$ Ω/m distributed uniformly along the wire; $l = 2$ μH/m; $c = 10$ pF/m; connection length $= 2$ m; therefore, L $= 4$ μH, C $= 20$ pF, and $Z_L = 1$ Ω.

Using these parameters, the characteristic impedance of the measuring transmission line at 1 MHz can be calculated to be $Z_0 \cong 1500e^{-j\pi/4}$ (it is even larger at lower frequencies). Given that $Z_L \ll |Z_0|$, it can be replaced by a short circuit for purposes of calculating the current through the load and hence the voltage across the 1-Ω measuring resistor. Hence, it is not necessary to know the actual value of Z_g as long as $|Z_g| \ll |Z_0|$. For these parameters, (23) is valid at frequencies below approximately 3 MHz.

[6]It will be shown shortly that the voltage across the 1-Ω shunt resistor is essentially independent of the total load impedance load.

The amplitude and phase of the transfer function can be respectively written as

$$|H(\omega)| \cong \frac{Z_L}{r\ell\left(1+\left(\frac{(\omega rc\ell^2)}{6}\right)^2\right)}, \quad \left(\omega rc\ell^2\right)/6 < 1 \tag{24}$$

$$\theta(\omega) \cong -\frac{\omega rc\ell^2}{6}. \tag{25}$$

It is well known that a transmission line does not distort the shape of a voltage wave traveling along if it has a transfer function of the form

$$H(\omega) = A\exp(-j\omega t_d) \tag{26}$$

where A is independent of frequency, and t_d is a time delay. Hence, for pulses with frequency content up to approximately 3 MHz, this measurement system is "distortionless" but results in a time delay of t_d seconds. This result justifies the term "constant transfer function" used by Grcev and Arnautovski-Toseva [42]. The time delay is

$$t_d = \frac{rc\ell^2}{6}. \tag{27}$$

For the parameters used in this experiment, this delay is 0.05 μs. This appears to be consistent with the slight delay in the measured voltage that will be observed later.

B. Special Cases for the Measured Voltage

Two cases will now be considered in order to explain how the voltage measured across the 1-Ω resistor ($\hat{V}_m(\omega)$) can be related to the voltage response of the ground system ($\hat{V}_{\rm GR}(\omega)$). The cases are for low and high frequencies, respectively. Before investigating these individual cases, it can be noted that $\hat{V}_m(\omega)$ can be calculated in terms of the voltage response of the ground system ($\hat{V}_{\rm GR}(\omega)$) using lossy transmission line theory, including the horizontal connection wire. However, this derivation assumes that there are no external voltages along the earth's surface that cause currents in the resistive divider. This is an important distinction between low- and high-frequency cases.

C. Measured Voltage: Low-Frequency Case

In the low-frequency case, the impedances of the measurement system's inductors (capacitors) are small (large) enough to be ignored compared with the other impedances in the network, as shown in Fig. 8. Furthermore, since the integral for the potential $\hat{\phi}_{WR}(\omega)$ does not converge before the reference point R, the rectangle is drawn to cover the entire measurement system as shown.

In this case, the voltages across the vertical and horizontal connections are zero, and the current through the resistances that compose the resistive divider is constant (i.e., no capacitive leakage) and equal to the current through the 1-Ω measurement resistor. Hence, this system can be analyzed using simple voltage divider theory. The result is

$$\hat{V}_m(\omega) = \frac{\hat{V}_{\rm GR}(\omega)}{r\ell+1} \cong \frac{\hat{V}_{\rm GR}(\omega)}{r\ell} \tag{28}$$

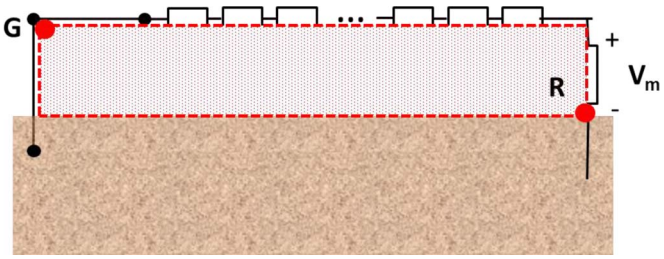

Fig. 8. Measurement system in the low-frequency case.

where r is the resistance per unit length of the divider, and ℓ is its length. This same result can be obtained from (23) in the limit as $f \to 0$. Hence, the measured voltage *at low frequencies* is

$$\hat{V}_{\rm GR}(\omega) = r\ell\hat{V}_m(\omega). \tag{29}$$

This low-frequency analysis is valid for frequencies such that the convergence of the potential integral occurs at a distance of more than 2 m from the point W. The highest frequency for which this occurs is approximately 500 kHz. For frequencies below this value, the transfer function is approximately constant, consistent with the dc analysis used to derive (29).

D. Measured Voltage: High-Frequency Case

At higher frequencies (i.e., 0.5 MHz or greater) for which the reactive elements cannot be ignored, it is no longer possible to use the simple model just analyzed. Rather, the measurement system will be represented by the transfer function given in (24) and (25). In order to use this result, however, it is first necessary to demonstrate that the only voltage source is the voltage across the 1-Ω resistor as assumed in its derivation. More specifically, it must be shown that there are no voltage sources along the surface of the earth that inject currents into the resistive divider.

In this high-frequency case, the potential integral $\hat{\phi}_{WR}(\omega)$ converges rapidly, and the point S can be considered to be its equivalent reference point. More specifically, the potential is

$$\hat{\phi}_{WR}(\omega) = -\int_R^W \overline{E}(\omega)\bullet\bar{d}\,\bar{l} \cong -\int_s^W \overline{E}(\omega)\bullet\bar{d}\,\bar{l} \cong \hat{\phi}_{Ws}(\omega). \tag{30}$$

Hence, the input voltage to the measurement system will be defined as $\hat{V}_{Gs}(\omega) \cong \hat{V}_{\rm GR}(\omega)$, where the voltage drop across the horizontal connecting wire is included. Hence, there are no significant voltages along the earth's surface between z = 0 and z = −15 m (see Fig. 9) that induce currents in the resistive divider, and it is legitimate to analyze it by assuming it is a passive network with a voltage source only at its input. The measurement system with a rectangle that illustrates this point is shown Fig. 9. Clearly, the measured voltage *at high frequencies* can be written as

$$\hat{V}_{\rm GR}(\omega) \cong \frac{\hat{V}_m(\omega)}{H(\omega)}. \tag{31}$$

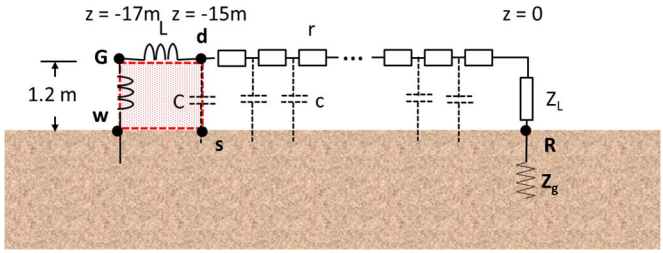

Fig. 9. Measurement system in the high-frequency case.

E. Measured Voltage: Full Frequency Range

The transfer function given in (24) and (25) reduces to the low-frequency result given in (28) for low frequencies. Hence, it can be used over the entire frequency range. Thus, the measured voltage can be written as

$$\hat{V}_{\mathrm{GR}}(\omega) \cong r\ell\left(1+\left(\frac{(\omega rc\ell^2)}{6}\right)^2\right)\exp\left(j\frac{\omega rc\ell^2}{6}\right)\hat{V}_m(\omega)$$
$$\cong r\ell\exp\left(j\frac{\omega rc\ell^2}{6}\right)\hat{V}_m(\omega)\ \left(\omega rc\ell^2\right)/6 \ll 1 \quad (32)$$

where the amplitude is constant, and the time delay is $t_d = (rc\ell^2)/6$.

VII. Approach to Modeling the Problem

A. Full-Wave High-Frequency Theories

The most accurate method for solving high-frequency grounding problems is to use full-wave theory for which no approximations are made to Maxwell's equations until numerical methods are employed. It is usually assumed that the earth is the lower half space and assumed to be linear, homogeneous,[7] and isotropic material characterized by the parameters ε_r (relative dielectric constant) and σ (conductivity). If it is assumed that there is a current (I_0) with a given frequency dependence, which is injected into the ground, then it is possible to set up an integral equation for the unknown current on the network of wires in the earth [14]. In the process of doing this, infinite Sommerfeld integrals are used to mathematically describe the electromagnetic fields of elementary current sources (i.e., Green's functions) in the earth that account for the electromagnetic discontinuity between the earth and the free space above it [45]. Generally, these equations are solved by the method of moments [16]. In this technique, the unknown wire currents are expanded using subsectional basis functions so that the wires are effectively divided into short elements with unknown currents. By matching boundary conditions on the wires in one of many appropriate methods and assuming that the input current is specified, a set of linear equations for the unknown currents is set up. These equations can be solved to find the distribution of current over the entire grounding network. Once this is done, it may be also possible to define a voltage and an input impedance, but care must be taken to interpret these correctly as discussed earlier.

If the response to a transient current is desired, then this can be calculated using the temporal inverse Fourier transform [14]. This is done by recognizing that, in a linear medium (as assumed until this point), Ampere's law, for example, in the time domain is written as

$$\nabla x\overline{H}(t) = \overline{J}_s(t) + \sigma\overline{E}(t) + \varepsilon_0\varepsilon_r\frac{\partial\overline{E}(t)}{\partial t} \quad (33)$$

where $\overline{J}_s(t)$ is the source current in the time domain. If the Fourier transform of (14) is taken, then it becomes

$$\nabla x\hat{\overline{H}}(\omega) = \hat{\overline{J}}_s(\omega) + (\sigma + j\omega\varepsilon_0\varepsilon_r)\,\hat{\overline{E}}(\omega) \quad (34)$$

where the carat "^" over a vector again indicates a phasor quantity. Equation (34) is the steady-state Maxwell's equation. Hence, if Maxwell's equations in the frequency domain are solved, the fields in the time domain can be found using the inverse Fourier transform as (for example)

$$\overline{E}(t) = \frac{1}{2\pi}\int_{-\infty}^{\infty}\hat{\overline{E}}(\omega)e^{-j\omega t}d\omega. \quad (35)$$

Here, the solution to this general problem will be applied to the specific EdF problem shown in Fig. 2 [14], [42], [45], [46].

VIII. Results

The system illustrated in Fig. 1 has been simulated in the frequency and time domains. The results of those simulations follow.

The simulated result without correction (i.e., $v_{WR}(t)$) was computed determining voltage between the conductor surface and a point 17 m away along a perpendicular path at the earth surface. The voltage was computed in the frequency domain by integrating the electric field vector along this path. This computation was repeated for a number of frequencies in a range from 0 Hz up to 5 MHz. To minimize the number of computations, only frequencies that allow evaluation of any required value by interpolation were directly computed. For the computation of such voltages as $V(\omega)$, steady-state 1-A excitation was used. The transient $v_{WR}(t)$ for a given current pulse $i(t)$ is obtained by Fourier transform technique, i.e.,

$$v_{WR}(t) = F^{-1}\left\{\hat{V}_{WR}(\omega)\cdot F\left[i(t)\right]\right\} \quad (36)$$

where $F(\ )$ and $F^{-1}(\ )$ are Fourier and inverse Fourier transforms, respectively. Practically discrete Fourier transform and standard fast Fourier transform algorithms are used (the interested reader may find details in [14]).

B. Voltage in the Frequency Domain

Fig. 10 shows a plot of the amplitude of the simulated voltage in the frequency domain with and without the inductive correction for the vertical wire as expressed in (13). The solid red line is the measured voltage after transformation into the

[7]The most common and relatively straightforward improvement of this model is to assume a multilayered earth.

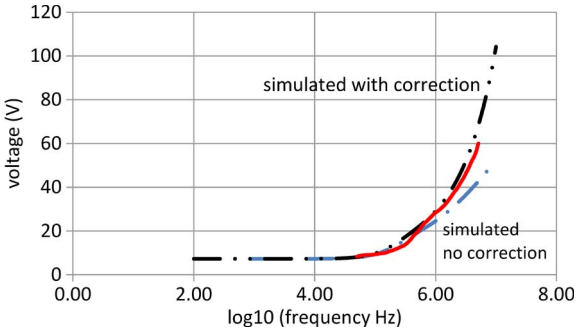

Fig. 10. Simulated voltage $\hat{V}_{\mathrm{GR}}$ in the frequency domain (with and without the inductive correction term) in comparison with the measured voltage (red).

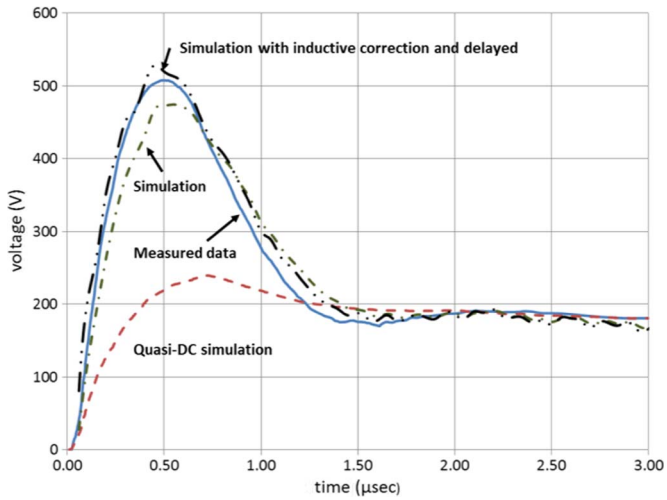

Fig. 11. Measurement and simulation (with and without inductive correction) of transient voltages to remote ground at the beginning point of 15-m-long horizontal wire. Shown also is the dc solution calculated from the grounding resistance of the buried electrode.

frequency domain. Clearly, the inductive correction term results in a better comparison with the measured results.

C. Voltage in the Time Domain

The result in the time domain is shown in Fig. 11. Here, the simulated voltage is presented in three forms. The first is the quasi-dc solution. The second is simply a plot of $\hat{\phi}_{WR}(\omega)$ transformed into the time domain. The third is the same result, but including the inductive correction term in (13) and the delay that is built into the transfer function of the distributed resistive divider indicated in (32).

Several observations can be made about these results. First, as aforementioned, the dc solution is clearly not acceptable in part because it does not account for inductive effects at early times. Second, the simulation without the aforementioned two corrections is fairly consistent with the measured results. However, when augmented by the inductive correction term and delayed by 0.05 μs, as required by the transfer function, the simulation is a very good replication of the experimental results.

IX. Discussion and Conclusion

The fact that the comparison between experiment and simulation is as close as shown in Fig. 11 is an illustration that it is possible to develop appropriate interpretable experiments for which ground systems are excited by currents with submicrosecond rise times and to develop appropriate full-wave methods for simulating these systems. However, it should be clear that the first of these cannot be completed without careful design and characterization of the measurement system to ensure that the meaning of the measurement is well understood. For example, mutual induction effects can be controlled by careful selection of geometry, and the transfer function of the measurement system should be characterized to be certain that distortion is minimized and inherent time delays accounted for. In addition, it should be clear that the specific simulation output required for comparison with the experiment should be carefully defined. For example, it may be necessary to account for inductance of measurement system wires in the simulation.

The fact that a satisfactory comparison has been obtained between experiment and full-wave theory for grounds excited by submicrosecond pulses does not necessarily mean that full-wave theory is required. However, the solution presented here can be used as a "gold standard" by which to measure the accuracy of techniques developed using assumptions other than full-wave solutions to Maxwell's equations.

References

[1] *IEEE Guide for Safety in AC Substation Grounding*, IEEE Std. 80-2000, May 2000.
[2] E. D. Sunde, *Earth Conduction Effects in Transmission Systems*, 2nd ed. New York, NY, USA: Dover, 1968.
[3] L. V. Bewley, *Traveling Waves on Transmission Systems*, 2nd ed. New York, NY, USA: Wiley, 1951.
[4] R. Rudenberg, *Electrical Shock Waves in Power Systems*. Cambridge, MA, USA: Harvard Univ. Press, 1968.
[5] R. Verma and D. Mukhedkar, "Impulse impedance of buried ground wire," *IEEE Trans. Power App. Syst.*, vol. PAS-99, no. 5, pp. 2003–2007, Sep./Oct. 1980.
[6] C. Mazzetti and G. M. Veca, "Impulse behavior of grounded electrodes," *IEEE Trans. Power App. Syst.*, vol. PAS-102, no. 9, pp. 3148–3156, Sep. 1983.
[7] R. Velazquez and D. Mukhedkar, "Analytical modeling of grounding electrodes," *IEEE Trans. Power App. Syst.*, vol. PAS-103, no. 6, pp. 1314–1322, Jun. 1984.
[8] A. Geri, "Behaviour of grounding systems excited by high impulse currents: The model and its validation," *IEEE Trans. Power Del.*, vol. 14, no. 3, pp. 1008–1017, Jul. 1999.
[9] A. F. Otero, J. Cidras, and J. L. del Alamo, "Frequency-dependent grounding system calculation by means of a conventional nodal analysis technique," *IEEE Trans. Power Del.*, vol. 14, no. 3, pp. 873–878, Jul. 1999.
[10] Y. Liu, N. Theethayi, and R. Thottappillil, "An engineering model for transient analysis of grounding system under lightning strikes: Nonuniform transmission-line approach," *IEEE Trans. Power Del.*, vol. 20, no. 2, pp. 722–730, Apr. 2005.
[11] P. Yutthagowith, A. Ametani, N. Nagaoka, and Y. Baba, "Application of the partial element equivalent circuit method to analysis of transient potential rises in grounding systems," *IEEE Trans. Electromagn. Compat.*, vol. 53, no. 3, pp. 726–736, Aug. 2011.
[12] D. Roubertou, J. Fontaine, J. P. Plumey, and A. Zeddam, "Harmonic input impedance of earth connections," in *Proc. IEEE Int. Symp. Electromagn. Compat.*, 1984, pp. 717–720.
[13] L. Grcev and Z. Haznadar, "A novel technique of numerical modelling of impulse current distribution in grounding systems," in *Proc. Int. Conf. Lightning Protect.*, Graz, Austria, 1988, pp. 165–169.
[14] L. Grcev and F. Dawalibi, "An electromagnetic model for transients in grounding systems," *IEEE Trans. Power Del.*, vol. 5, no. 2, pp. 1773–1781, Oct. 1990.
[15] R. Olsen and M. C. Willis, "A comparison of exact and quasi-static methods for evaluating grounding systems at high frequencies," *IEEE Trans. Power Del.*, vol. 11, no. 2, pp. 1071–1081, Jul. 1996
[16] R. F. Harrington, *Field Computation by Moment Methods*. Piscataway, NJ, USA: IEEE Press, 1993.

[17] P. L. Bellaschi, "Impulse and 60-cycle characteristics of driven grounds," *AIEE Trans.*, vol. 60, no. 3, pp. 123–128, Mar. 1941.
[18] P. L. Bellaschi, R. E. Armington, and A. E. Snowden, "Impulse and 60-cycle characteristics of driven grounds-II," *AIEE Trans.*, vol. 61, no. 6, pp. 349–363, Jun. 1942.
[19] K. Berger, "The behavior of earth connections under high intensity impulse currents," in *Proc. CIGRE*, 1946, vol. 95, pp. 1–32.
[20] A. C. Liew and M. Darveniza, "Dynamic model of impulse characteristics of concentrated earths," *Proc. Inst. Elect. Eng.*, vol. 121, no. 2, pp. 123–135, Feb. 1974.
[21] Saint-Privat-d'Allier Research Group, "Eight years of lightning experiments at Saint-Privat-d'Allier," *Rev. Gen. l'Elect.*, vol. 91, pp. 561–582, Sep. 1982.
[22] S. Bourg, B. Sacepe, and T. Debu, "Deep earth electrodes in highly resistive ground: Frequency behaviour," in *Proc. IEEE Int. Symp. Electromagn. Compat.*, 1995, pp. 584–589.
[23] Z. Stojkovic, M. S. Savic, J. M. Nahman, D. Salamon, and B. Bukorovic, "Sensitivity analysis of experimentally determined grounding grid impulse characteristics," *IEEE Trans. Power Del.*, vol. 13, no. 4, pp. 1136–1142, Oct. 1998.
[24] S. Sekioka, H. Hayashida, T. Hara, and A. Ametani, "Measurements of grounding resistances for high impulse currents," *Proc. Inst. Elect. Eng.—Gen., Transmiss. Distrib.*, vol. 145, no. 6, pp. 693–699, Nov. 1998.
[25] H. M. Towne, "Impulse characteristics of driven grounds," *Gen. Elect. Rev.*, vol. 32, no. 11, pp. 605–609, Nov. 1929.
[26] M. Nor, A. Haddad, and H. Griffiths, "Factors affecting soil characteristics under fast transients," in *Proc. Int. Conf. IPST*, New Orleans, LA, USA, 2003, pp. 1–6.
[27] F. Asimakopoulou, I. F. Gonos, and I. A. Stathopulos, "Methodologies for determination of soil ionization gradient," *J. Electrostat.*, vol. 70, no. 5, pp. 457–461, Oct. 2012.
[28] A. M. Mousa, "The soil ionization gradient associated with discharge of high currents into concentrated electrodes," *IEEE Trans. Power Del.*, vol. 9, no. 3, pp. 1669–1677, Jul. 1994.
[29] V. Cooray, "Soil ionization," in *Lightning Protection*, V. Cooray Ed. London, U.K.: Inst. Eng. Technol., 2010, pp. 531–552.
[30] L. Grcev, "Time-and frequency-dependent lightning surge characteristics of grounding electrodes," *IEEE Trans. Power Del.*, vol. 24, no. 4, pp. 2186–2196, Oct. 2009.
[31] H. Rochereau, "Response of earth electrodes when fast fronted currents are flowing out," in *EdF Bull. la Direction des Etudes et Recherches*, ser. B, no. 2, 1988, pp. 13–22.
[32] B Merheim, "Modellierung von hochspannungs-erdersystemen und vergleich mit messungen ihres dynamischen verhaltens," Dipl.Ing. thesis (in English), Diplomaufgabe, Inst. Allgemeine Hochspannungstechnik, Technischen Hochschule, Aachen, Germany, 1992.
[33] H. Rochereau and B. Merheim, "Application of the transmission lines theory and EMTP program for modelisation of grounding systems in high frequency range," in *Collection de notes internes de la Direction des Etudes et Recherches Electricité de France*, vol. 93NR00059, Paris, France, May 1993, pp. 1–31.
[34] R. Fieux, P. Kouteynikoff, and F. Villefranque, "Measurement of the impulse response of groundings to lightning currents," in *Proc. 15th Int. Conf. Lightning Protect.*, Uppsala, Sweden, 1979.
[35] F. Villefranque, "Comportment de differentes prises de terre reelles parcourues par des courants impulsionnels differentes durees de front," Elect. France Res., Clamart, France, Rep. 645 21.64, Feb. 8, 1978.
[36] A. P. Meliopoulos, R. P. Webb, and E. B. Joy, "Analysis of grounding systems," *IEEE Trans Power. App. Syst.*, vol. PAS-100, no. 3, pp. 1039–1048, Mar. 1981.
[37] R. P. Nagar, R. Velazquez, M. Loeloeian, D. Mukhedkar, and Y. Gervais, "Review of analytical methods for calculating the performance of large grounding electrodes—Part I: Theoretical considerations," *IEEE Trans. Power App. Syst.*, vol. PAS-104, no. 11, pp. 3124–3133, Nov. 1985.
[38] M. Loeloeian, R. Velazquez, and D. Mukhedkar, "Review of analytical methods for calculating the performance of large grounding electrodes—Part II: Numerical results," *IEEE Trans. Power App. Syst.*, vol. PAS-104, no. 11, pp. 3134–3141, Nov. 1985.
[39] L. Grcev and M. Popov, "On high-frequency circuit equivalents of a vertical ground rod," *IEEE Trans. Power Del.*, vol. 20, no. 2, pp. 1598–1603, Apr. 2005.
[40] L. Grcev, B. Markovski, and S. Grceva, "On inductance of buried horizontal bare conductors," *IEEE Trans. Electromagn. Compat*, vol. 53, no. 4, pp 1083–1087, Nov. 2011
[41] L. Grcev, "Lightning surge efficiency of grounding grids," *IEEE Trans. Power Del.*, vol. 26, no. 3, pp. 1692–1699, Jul. 2011.
[42] L. Grcev and V. Arnautovski-Toseva, "Grounding systems modeling for high frequencies and transients: Some fundamental considerations," in *Proc. IEEE Bologna Power Tech Conf.*, Bologna, Italy, Jun. 23–26, 2003, pp. 1–7.
[43] L. Grcev, "Computer analysis of transient voltages in large grounding systems," *IEEE Trans. Power Del.*, vol. 11, no. 2, pp. 815–823, Apr. 1996.
[44] R. C. Dorf, *Handbook of Engineering Tables*. Boca Raton, FL, USA: CRC Press, 1962
[45] A. Banos, *Dipole Radiation in the Presence of a Conducting Half-Space*. New York, NY, USA: Pergamon, 1966.
[46] L. Grcev and M. Heimbach, "Frequency dependent and transient characteristics of substation grounding systems," *IEEE Trans. Power Del.*, vol. 12, no. 1, pp. 172–178, Jan. 1997.
[47] M. Heimbach and L. Grcev, "Grounding system analysis in transients programs applying electromagnetic field approach," *IEEE Trans. Power Del.*, vol. 12, no. 1, pp. 186–193, Jan. 1997.

Robert G. Olsen (S'66–F'92) received the B.S.E.E. degree from Rutgers University, New Brunswick, NJ, USA, in 1968 and the M.S. and Ph.D. degrees from the University of Colorado, Boulder, CO, USA, in 1970 and 1974, respectively.

Since 1973, he has been with Washington State University, Pullman, WA, USA. His other positions have included Senior Scientist with Westinghouse Georesearch Laboratory; NSF Faculty Fellow with GTE Laboratories; Visiting Scientist with ABB Corporate Research and the Electric Power Research Institute (EPRI); and Visiting Professor with the Technical University of Denmark, Kongens Lyngby, Denmark. His work has resulted in approximately 85 and 150 publications in refereed journals and conference proceedings, respectively. He is one of the authors of *AC Transmission Line Reference Book—200 kV and Above*, which is published by EPRI. His research interest is the application of electromagnetic theory to high-voltage power transmission systems.

Dr. Olsen is an Honorary Life Member of the IEEE Electromagnetic Compatibility Society. He has been a U.S. National Committee Representative to CIGRE Study Committee 36 (Electromagnetic Compatibility) and a Chair of the IEEE Power Engineering Society AC Fields and Corona Effects Working Groups. He has been also an Associate Editor of the IEEE TRANSACTIONS ON ELECTROMAGNETIC COMPATIBILITY AND RADIO SCIENCE.

Leonid Grcev (M'84–SM'97–F'13) received the Dipl.-Ing. degree from Ss. Cyril and Methodius University, Skopje, Macedonia, in 1978 and the M.S. and Ph.D. degrees from the University of Zagreb, Zagreb, Croatia, in 1982 and 1986, all in electrical engineering.

From 1978 to 1988, he was with the Electric Power Company of Skopje, working in the Telecommunications Department. He is currently a Professor with the Faculty of Electrical Engineering and Information Technologies, Ss. Cyril and Methodius University, where he has also held the positions of Assistant Professor, Associate Professor, and Vice Dean since 1988. He has been a Visiting Professor with the Technical University of Aachen, Aachen, Germany; Eindhoven University of Technology, Eindhoven, The Netherlands; and the Swiss Federal Institute of Technology in Lausanne, Lausanne, Switzerland. He was responsible for several international projects related to electromagnetic compatibility (EMC). He has authored or coauthored many scientific papers published in peer-reviewed journals and presented at international conferences. He is the principal author of TRAGSYS software for transient analysis of grounding systems. His research interests include EMC, lightning, and electromagnetic modeling of high-frequency and transient grounding.

Dr. Grcev has been a member of the CIGRE Working Groups related to EMC and lightning protection and has served as the Chairperson and as a member of scientific committees at international conferences. He is a member of the Macedonian Academy of Sciences and Arts.